

PRESSURE DROP ACROSS A FIXED
BED OF ION-EXCHANGE RESIN

by

James G. Ling

A Thesis Submitted to the
Graduate Faculty in Partial Fulfillment of
The Requirements for the Degree of
MASTER OF SCIENCE

Major Subject: Nuclear Engineering

Signatures

Signatures have been redacted for privacy

Iowa State University
Of Science and Technology
Ames, Iowa

1959

TABLE OF CONTENTS

	Page
I. ABSTRACT	1
II. INTRODUCTION	2
III. LITERATURE SURVEY	4
IV. APPARATUS	9
V. PROCEDURE	21
VI. RESULTS AND DISCUSSION	22
A. Gauge Pressure in the Column	22
B. Variation of Bed Height with Flow Rate	27
C. Reproducibility of Data	27
D. Pressure Drop Across the Bed	32
E. Variation of Pressure Drop with pH	39
VII. CONCLUSIONS AND RECOMMENDATIONS	48
VIII. BIBLIOGRAPHY	50
IX. APPENDIX	52
A. Sample Calculations	52
B. Data for Graphs	54

I. ABSTRACT

Pressure drop across a fixed bed of ion-exchange resin was measured at different flow rates and pH values. The resin used was Dowex 50W-X2, H+ form, 50-100 mesh. Measurements were made in a Lucite column, 3.50 inches in inside diameter, 52 inches high, with a resin bed 30 inches deep.

The resin bed was compressible and became more tightly packed as flow rate increased. About 15 minutes were required for the packed bed to become stabilized at each new flow rate.

The average pressure drop of distilled water across the bed increased with flow rate between 0 and 300 cubic centimeters per minute according to the equation:

$$\frac{\Delta P}{L} = 2.27 \times 10^{-3} v$$

where $\frac{\Delta P}{L}$ = pressure drop per unit height of packing, in pounds per square inch per foot of resin,

v = fluid velocity, in cubic centimeters per minute.

The pressure drop per foot of resin increased slightly as pH was decreased. There was no visible change in shape of the resin with changing pH. The increased pressure drop was probably caused by increased viscosity.

II. INTRODUCTION

Ion exchange using naturally occurring zeolites has been used in water softening for many years. The development of synthetic organic exchangers by Adams and Holmes in 1935 greatly increased the potential of ion exchange as a chemical processing unit operation. During the past ten years ion exchange has taken its place among traditional unit operations such as distillation, absorption, and extraction. At present a variety of "tailor-made" synthetic ion exchangers are widely used in both chemical and nuclear industries. Interest in ion exchange is increasing as more of its potentials are discovered.

Ion exchange is still used most extensively for water softening. Its industrial uses include purification of chemicals, recovery of small amounts of valuable substances and separation of ion mixtures.

The applications of ion exchange in the nuclear engineering field are:

1. Recovery of uranium from low-grade ore
2. Purification of cooling water for nuclear power reactors
3. Treatment of radioactive wastes
4. Separation of rare earth elements

The current trend in ion exchange technology is toward continuous processes using moving-bed equipment. However, most ion exchange installations are still of the fixed-bed type. The physical behavior of ion exchange beds is not completely understood. In particular, it is difficult to scale-up an ion exchange unit from a laboratory model. This study on pressure drop across a fixed bed of ion-exchange resin was aimed at isolating some of the variables in the system. The variables considered here were:

1. The effect of time on pressure drop
2. The effect of flow rate on pressure drop
3. The effect of pH on pressure drop

The resin used in this study was Dowex 50W-X2, H⁺ form, 50-100 mesh.

It is a strongly acidic cation exchange resin of the form (RSO₃)H. The measurements were made on pilot plant scale equipment.

III. LITERATURE SURVEY

The general subject of ion-exchange resins will not be treated here. The most comprehensive bibliography on ion-exchange resins is published by the Office of Technical Services, U.S. Department of Commerce (17).

Fluid flow through packed beds has been studied in such fields as chemical engineering, civil engineering, mechanical engineering, hydrodynamics and others. Pressure drop through a packed system is determined by many variables, and early studies dealt with one or two variables, assuming the others to be constant. The most recent works on this subject have attempted to recognize and correlate all the variables.

In 1856 D'Arcy (9) proposed that the pressure drop per unit length of a porous bed was proportional to the flow of water through it. This could be expressed by the equation:

$$U = K \frac{\Delta P}{L}$$

where U = average linear fluid velocity,

ΔP = pressure drop across the entire bed,

L = height of the packed bed,

K = proportionality constant.

The D'Arcy equation was modified in 1863 by Dupuit (11) who suggested that the liquid velocity was also a function of the porosity, ϵ , of the bed.

The modified D'Arcy equation is:

$$U = \frac{\epsilon K \Delta P}{L}$$

In 1914, Boussinesq (3) (4) derived theoretical formulas similar to those of D'Arcy and Dupuit. Porosity was also considered by Chalmers, Taliaferro, and Rawlins (6) in 1932. They defined the friction factor, f , in the case

of gas flow as:

$$f = \frac{\Delta P D_p g_c \epsilon^2}{\rho L U^2}$$

where D_p = diameter of packing particle,

g_c = conversion factor, 4.17×10^8 ft. per hour per hour,

ρ = fluid density.

In 1939, Hatfield (16) studied the viscous flow of gases and liquids through porous carbon and defined the friction factor in the same manner as Chalmers et al. This friction factor was a linear function of the Reynolds number in the flow range $10^{-5} < Re < 10^2$.

Meyer and Work (23) defined D_p as:

$$D_p = \sum w_i D_i$$

where w_i = weighting factor,

D_i = diameter of particle.

They obtained the pressure drop relationship:

$$\frac{\Delta P}{L} = \frac{K \mu (67 - \epsilon)}{g (D_p - \frac{\epsilon}{\epsilon_n})^2}$$

where μ = fluid viscosity,

ϵ_n = bed voidage for the loosest packing available for the specific material.

Meanwhile other investigators ignored the effect of porosity. In 1925, von Emmerleben (26) used hydrodynamic principles to derive the D'Arcy equation. Fancher and Lewis (13) studied the flow of air, water and crude petroleum through beds of sands, sandstones, and lead shot in 1933. Their value of f in the viscous range was:

$$f = \frac{\Delta P D_p g_c}{2 \rho L U^2}$$

Fancher and Lewis defined D_p as:

$$D_p = \left(\frac{\sum n D_i}{\sum n} \right)^{1/3}$$

where D_p = diameter of average grain,

n = number of particles of any size D_i .

Later White (28) attempted to correlate data of other investigators for ring-and saddle-packed beds by defining f as:

$$f = \frac{\Delta P_p D_p}{2 \rho U^2 L F_a}$$

where F_a = empirical correction factor dependent on particle size.

The effect of particle shape on pressure drop was also the subject of several studies. Blake (2) studied the effects of glass cylinders, Raschig rings, and crushed pumice and obtained a linear log-log plot of:

$$\frac{\Delta P \rho \epsilon^3}{L G^2 S} \text{ vs. } \frac{G}{\mu S}$$

where S = surface area of packing per unit volume of packed tube,

G = fluid mass velocity.

Furnas (14) studied the effect of several variables and published the equation:

$$\frac{\Delta P}{L} = A G^B$$

where A and B = complex functions of particle size, bed porosity, temperature, viscosity, density, and molecular weight.

In 1934, Wadell (27) studied the coefficient of resistance for solids of various shapes. He defined a shape factor as the ratio of the surface of a sphere having the same volume of the particle to the actual surface of the particle. Chilton (7) later correlated the data of White (28) and Zeisberg (29) to compute friction factors for various shapes. These friction

factors could be used in the previously published Chilton-Colburn equation (8):

$$\frac{\Delta P}{L} = \frac{2fG^2 A_f}{\epsilon_c D_p \rho}$$

where A_f = wall-effect factor.

In 1937, Carman (5) published a correlation which was especially applicable to beds of abnormal void content. The Carman equation is:

$$f = \frac{\Delta P g_c \epsilon^3}{L \rho u^2 S_1}$$

where $S_1 = S + \frac{4}{Dt}$,

Dt = diameter of vessel holding the packed bed.

Hatch (15) investigated pressure drops in packed tubes and developed the dimensionally homogeneous equation:

$$\frac{h}{l} = \frac{k}{\epsilon_c} \left(\frac{\mu}{\rho} \right)^{2-n} \left[u^n \left(\frac{A_p}{V_p} \right)^{3-n} \right] \left[\frac{(1-\epsilon)^{3-n}}{\epsilon^3} \right]$$

where $\frac{h}{l}$ = resistance per length of bed,

k = a coefficient,

n = state of flow factor,

A_p = surface area of a sphere of equivalent volume,

V_p = solid volume of one individual packing element.

In 1951, Leva et al. (21) derived the working equation:

$$\Delta P = \frac{k}{\epsilon_c} \left(\frac{D_p G}{\mu} \right)^n \left(\frac{\mu^2}{\rho} \right) \left(\frac{\lambda}{D_p^3} \right)^{3-n} \frac{(1-\epsilon)^{3-n}}{\epsilon^3}$$

where μ = fluid viscosity,

λ = particle shape factor.

The equation was modified for turbulent, laminar, and transitional flow by evaluating the experimental constants in each case.

Ergun (12) developed a gas flow method for determining the particle density of crushed porous materials from gas flow rate, pressure drop, and bulk density measurements.

In 1951, Martin, McCabe, and Monrad (22) studied the effect of orientation on pressure drop through stacked spheres. They suggested that orientation differences can account for the variation in pressure drop through beds of particles of the same diameter and shape packed to the same porosity.

In 1953, Schwartz and Smith (25) showed that the velocity across the diameter of a packed bed was not uniform. Data obtained in pipe sizes from 2 to 4 inches indicated that a peak velocity occurred about one pellet diameter away from the pipe wall.

In 1957, Leva (18) (19) (20) summarized current information on flow through packings and beds. For predicting pressure drop he used the Kozeny-Carman type equation:

$$\Delta P = \frac{2fg^2L(1-\epsilon)^{3-n}}{D_p \phi_s^{3-n} \epsilon^3 g_c \rho}$$

where ϕ_s = bed shape factor.

This equation applies to almost the entire flow range. It is adapted to a particular flow range by substituting the appropriate value of the state of flow factor n .

IV. APPARATUS

The ion-exchange column used in this study was part of an ion-exchange system consisting of two cylindrical Lucite columns. Each column was 52 inches long and 4.00 inches in outside diameter. The columns were fed from a head tank which was supplied by two feed tanks. Product from the columns passed through rotameters and could be discharged, collected, recycled, or fed to another column in series.

The column was made of one standard 52-inch length of Lucite pipe, 4.00 inches in outside diameter and 3.50 inches in inside diameter. The bottom was cemented to a Lucite disc through which two Type 316 stainless steel bulkhead unions were fitted. The top of the column fitted against a soft polyethylene disc drilled for a single drain outlet. Both ends were capped by plywood blocks, 8.0 inches square and $1\frac{1}{4}$ inch thick. The entire assembly was held in compression by four $\frac{3}{8}$ inch steel rods, 55 inches long, threaded and bolted at their ends. The column assembly was mounted on a steel rack 30 inches above the ground floor.

A $\frac{1}{4}$ inch thick Lucite ring, $1\frac{1}{2}$ inches high and $3\frac{1}{2}$ inches in outside diameter, rested on the bottom of the column. A perforated polyethylene disc, $\frac{1}{4}$ inch thick and $3\frac{1}{2}$ inches in outside diameter, rested on the Lucite ring and supported the resin bed. A 180-mesh stainless steel screen soldered to a 30-mesh stainless steel screen covered the polyethylene disc.

The two bulkhead unions at the bottom of the column were fitted to stainless steel tubing. One line carried effluent to a pump from which it passed through a settler to a rotameter. The other line served as a bottom drain and as an inlet for the backwash stream.

Feed entered the column through a distributor 2 inches from the top. The distributor was made of welded 20-gauge Type 316 stainless steel tubing, $\frac{3}{8}$ inch in outside diameter and 0.305 inch in inside diameter. Five outlet holes $\frac{3}{22}$ inch in diameter were evenly spaced along the length of the tube, and the tube was wrapped with a 30-mesh stainless steel screen. The distributor was perpendicular to the longitudinal axis of the column with feed entering from the front. It was held in place by two stainless steel male connectors which were screwed into the column and drilled out to allow passage of the tube. Four pressure taps were installed along the bottom half of the column. The taps consisted of male tubing fittings screwed into the side of the column. A 180-mesh stainless steel screen was soldered over the opening of each fitting on the end which contacted the resin.

The feed tanks were two Type 316 stainless steel 55-gallon drums mounted 8 inches above the ground floor on a steel rack. A series of valves permitted feed from one tank at a time or from both tanks simultaneously. An overflow line from the head tank entered each feed tank through the center of the cover.

The head tank was made of a 12-inch section of Lucite pipe, 4.00 inches in outside diameter and 3.50 inches in inside diameter. The bottom was cemented to a Lucite disc through which two stainless steel bulkhead unions were fitted. One fitting was attached to the inlet line from the feed pump. The other fitting was attached to the line which fed the ion-exchange columns. The top of the head tank fitted against a soft polyethylene disc which had a center-drilled vent hole. Both ends of the head tank were capped by wood blocks, 8.0 inches square and $1\frac{1}{4}$ inch thick. The assembly

was held in compression by 3/8-inch steel rods, 15 inches long, threaded and bolted at the ends. The tank was mounted on a steel bracket which was level with the second floor. An overflow line returning to the feed tanks was attached to a male fitting which was screwed into the side of the head tank.

A 500-millimeter glass suction flask served as a settler between the product pump and rotameter. Flexible Tygon tubing was used for temporary connections between the settler and rotameter.

Fluid flow was measured with either of two Brooks rotameters, one providing a range of 25 to 300 cubic centimeters per minute of liquid with specific gravity of 1.0, and the other providing a range of 0.1 to 0.59 gallon per minute.

Pressure in the column was measured with two open-end U-tube glass manometers. The top three taps were connected to one manometer through a stainless steel manifold. The connections were made with flexible Tygon tubing which could be closed with pinch clamps. The bottom pressure tap was connected directly to the second manometer. The manometer fluid was methylene bromide dyed with Red Sudan which colored the organic phase but not the aqueous. The original manometer fluid, mercury, was not sensitive enough to small changes in pressure. Carbon tetrachloride, specific gravity 1.595, was not heavy enough as a manometer fluid to balance the static head in the column. Methylene bromide, specific gravity 2.495, was sensitive to small pressure changes and also heavy enough to balance the static head.

All metal parts which contacted the process stream were made of Type 316 stainless steel. All tubing was welded 20-gauge Type 316 stainless steel, 3/8 inch in outside diameter and 0.305 inch in inside diameter. The

tube fittings were Parker Triple-Lok fittings. Hoke Model Y343H needle valves with vee spindles were used for close flow control. Hoke Model PY276 valves with blunt spindles were used where fully open or closed operation was required.

All pumps in the system were Eastern Industries Model E-1 pumps with Type 316 stainless steel construction and mechanical seals. These pumps were driven by 1/15 horsepower electric motors.

Figure 1. Ion Exchange Unit



Figure 2. Close-up of Ion Exchange Columns

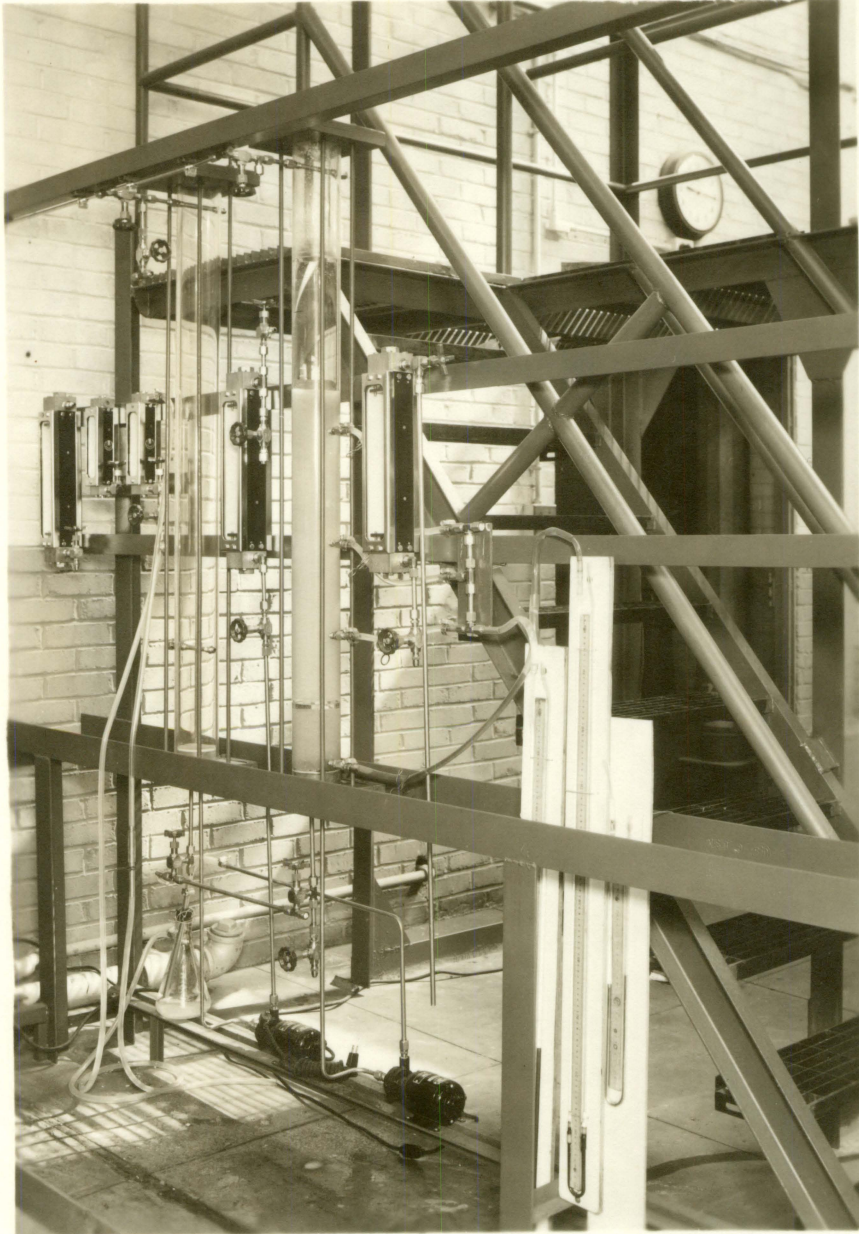
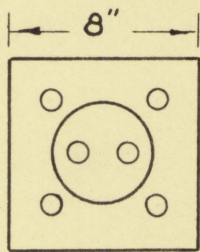
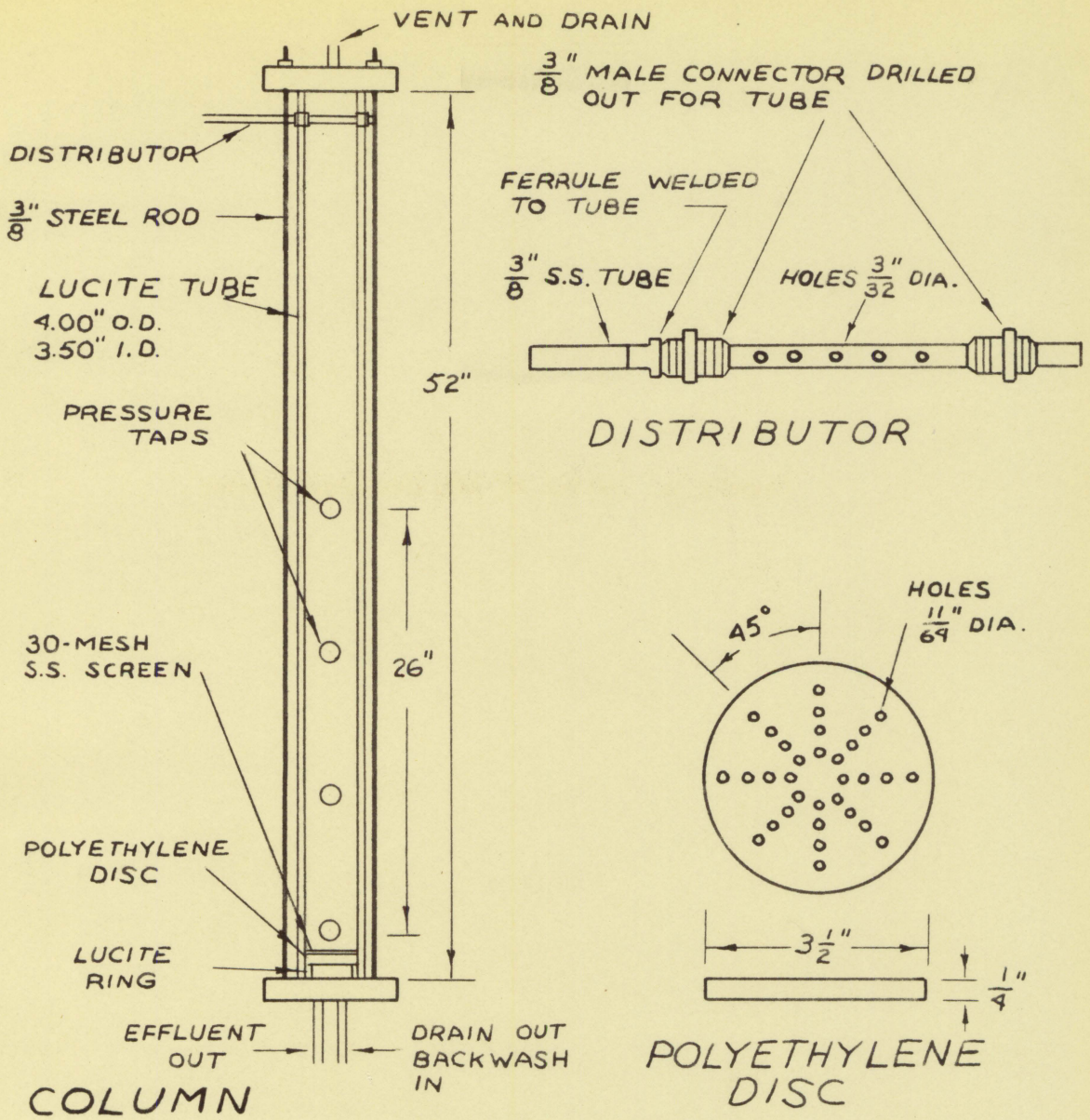
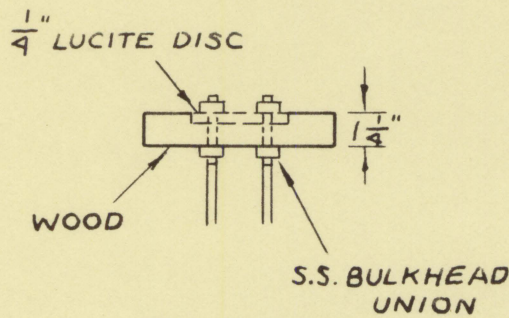


Figure 3. Detail of Ion Exchange Column

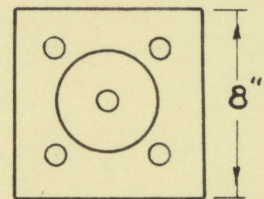
Figure 3. Detail of Ion Exchange Column



BASE

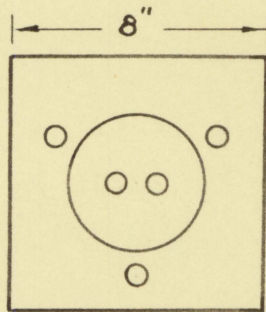
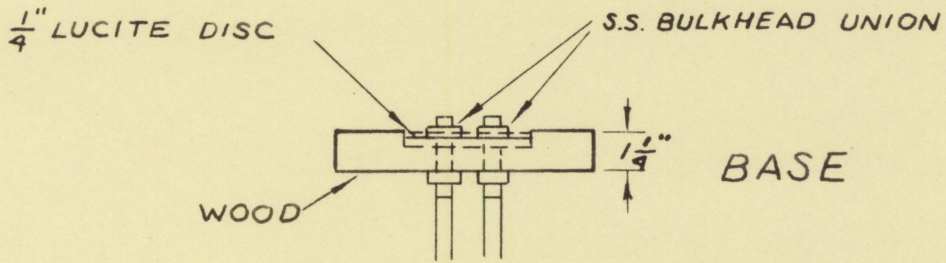
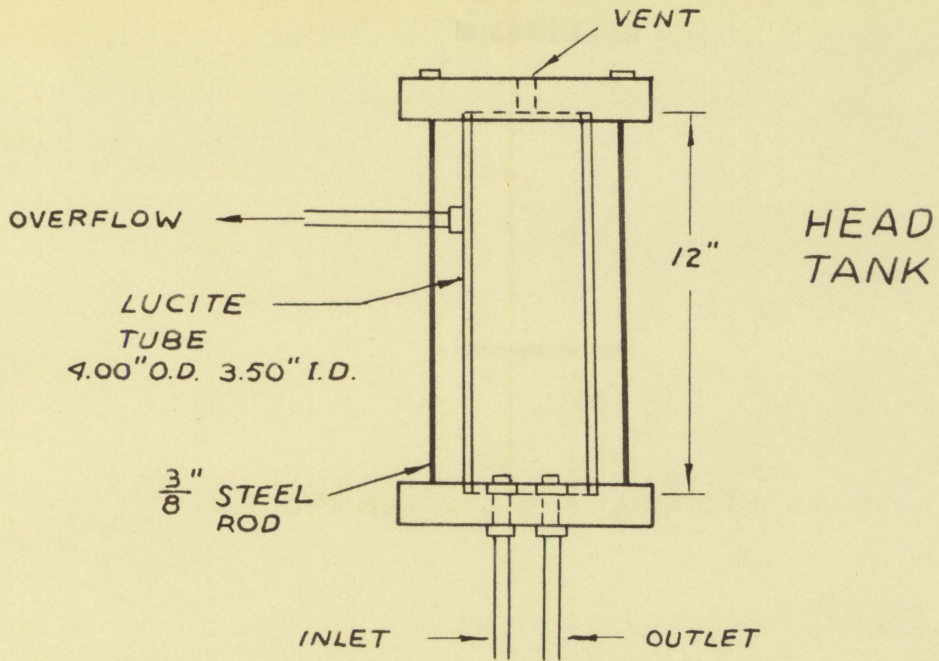


BASE

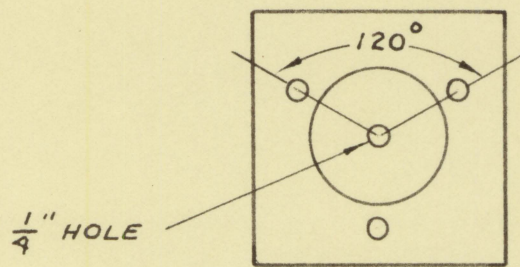


TOP

Figure 4. Detail of Head Tank



BASE



TOP

V. PROCEDURE

The column was charged with ion-exchange resin to about half its height. The resin bed was then backwashed with distilled water from the feed tank. The backwash rate was controlled so that the liquid level in the column rose about one inch per minute. When the liquid level reached the feed distributor backwashing was stopped and the particles were allowed to settle for at least one hour.

When the particles had settled the feed pump was turned on and liquid was circulated from the feed tank through the head tank and the overflow line. When the liquid head was constant the product pump was turned on and the needle valve adjusted to obtain the desired product flow rate. The feed valve was adjusted to maintain a constant height of liquid in the column. Once the operation reached steady state the manometer hose clamps were removed to obtain the desired pressure readings.

The pH of the feed was lowered by adding concentrated sulfuric acid to distilled water in the feed tank.

VI. RESULTS AND DISCUSSION

A. Gauge Pressure in the Column

The gauge pressure at four points in the column was measured by open-end U-tube manometers filled with methylene bromide.¹ The graphs in figure 5 show gauge pressure in the column as a function of distance above the bottom pressure tap. In this series the liquid flowed through the column under the force of gravity. With no flow the pressure at the sample points was simply that of the static liquid head. The pressure was thus a linear function of distance from the bottom tap. Gauge pressure was about 1.33 pounds per square inch at the bottom pressure tap and 0.37 pounds per square inch at the top tap.

As liquid flowed through the bed the pressure at all taps decreased by an amount proportional to the frictional loss of energy. The frictional loss was proportional to the height of packing through which the liquid passed. Therefore, the pressure at the bottom tap dropped rapidly with increasing flow, and the slope of the pressure curve at 262 cubic centimeters per minute was almost the reverse of that at no flow. The non-linear characteristic of the graphs was probably caused by non-uniform packing of the bed as flow was increased. Pressure at the top tap dropped initially then stayed almost constant at flow rates greater than 150 cubic centimeters per minute.

The graphs in Figure 6 show pressure distribution in the column when liquid was drawn through the bed by a pump. The pressure drop per foot of

¹See sample calculations in Appendix A.

Figure 5. Pressure vs. Distance from Bottom Tap for Gravity
Flow of Distilled Water Across Dowex 50W-X2, 50-100 Mesh

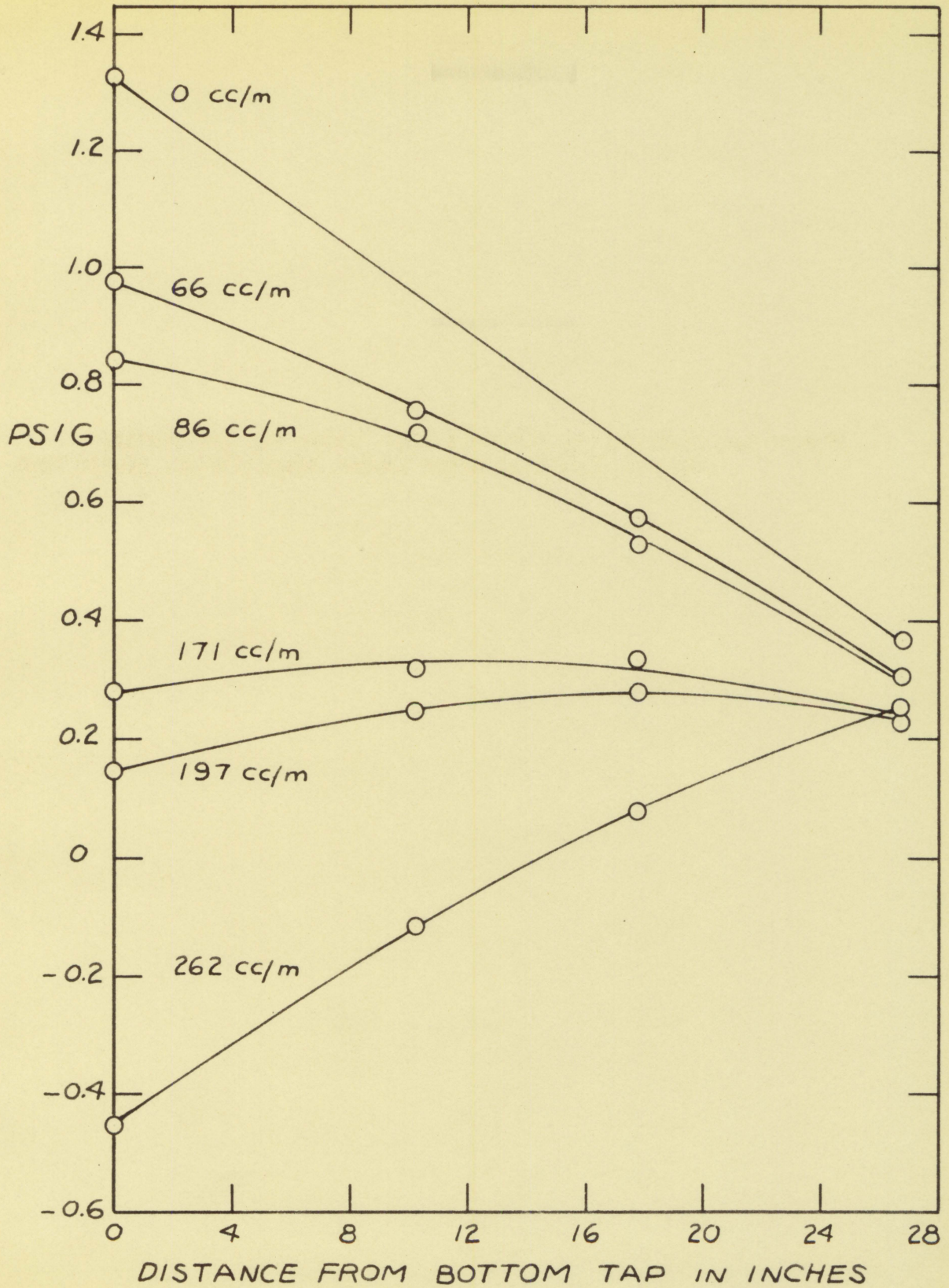
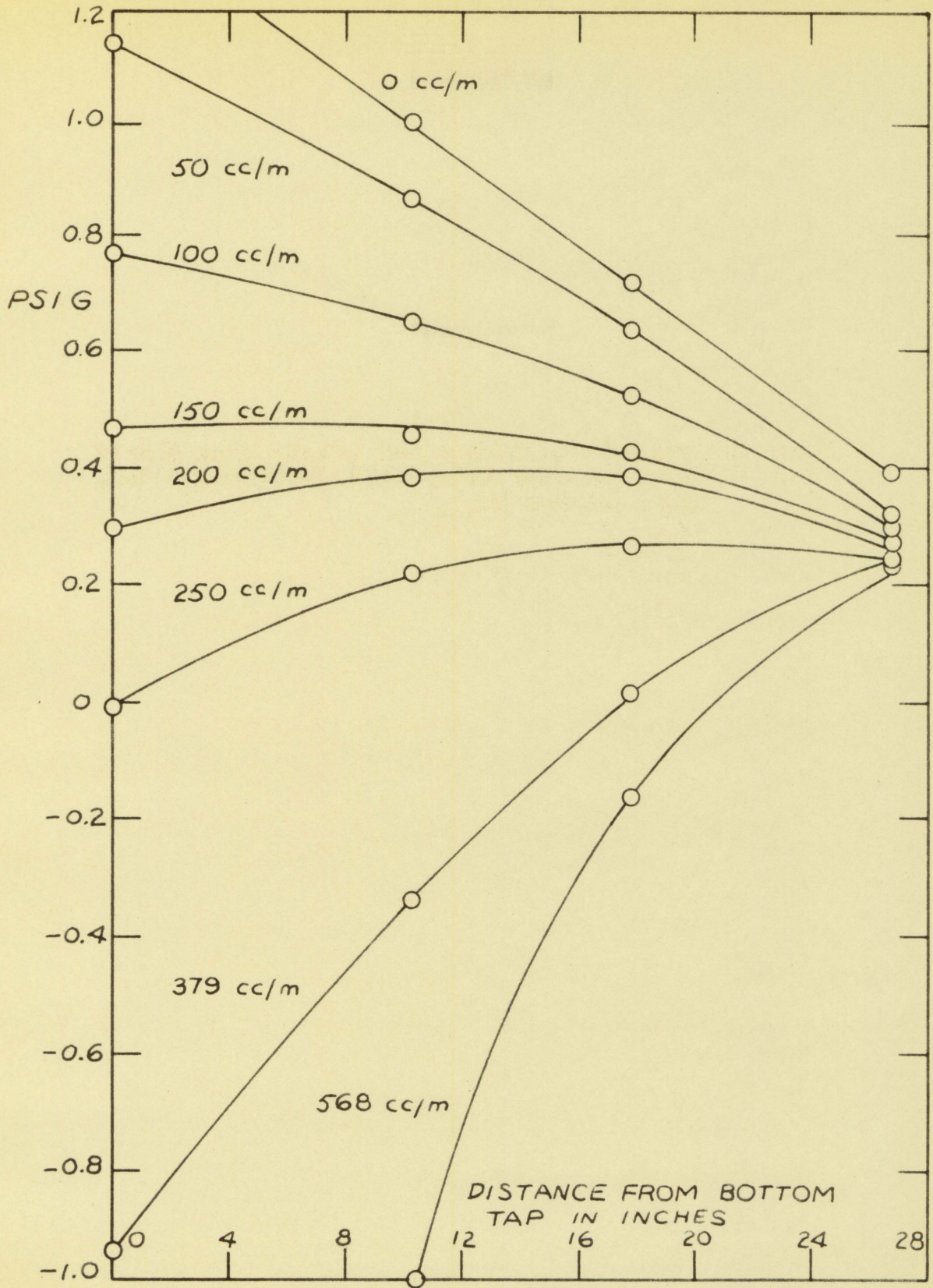


Figure 6. Pressure vs. Distance from Bottom Tap for Flow of Distilled Water Across Dowex 50W-X2, 50-100 Mesh, Using Effluent Pump



resin was the same as with gravity flow. The pressure curves also have the same shape. The maximum flow rate obtainable in the column with 50-100 mesh resin was 0.15 gallon per minute or 568 cubic centimeters per minute.

B. Variation of Bed Height with Flow Rate

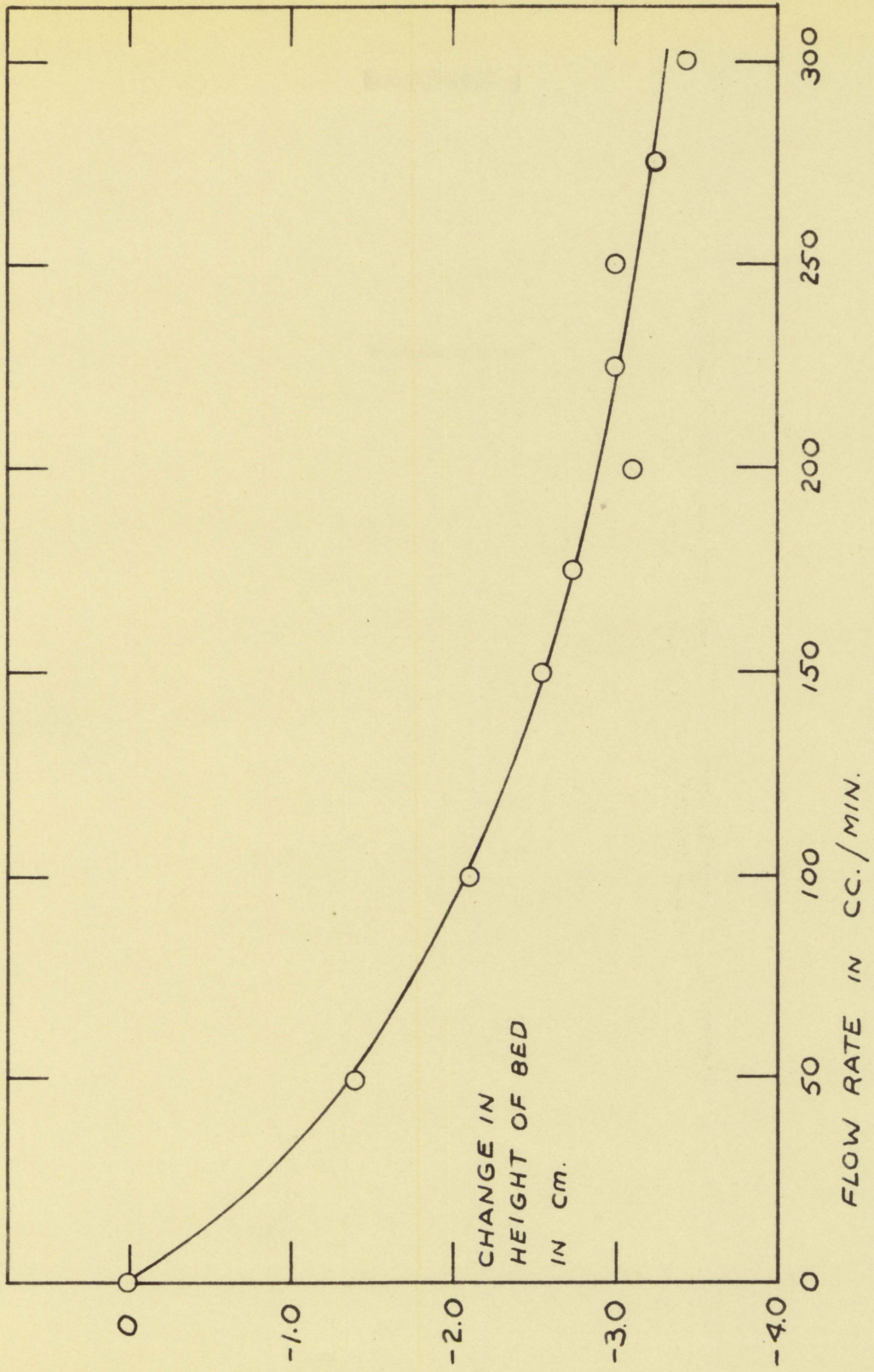
The ion-exchange column was backwashed slowly with distilled water before each run to re-classify the resin bed and establish random arrangement of the particles. Once the particles had settled and liquid was passed through the column there was a further compression of the bed. The graph in Figure 7 shows change in height of the resin bed as a function of flow rate. The height of the bed decreased rather rapidly at low flow rates and gradually approached a constant as flow was increased. When flow was decreased the bed expanded with very little residual effect from the compression.

The resin in the bed was Dowex 50W-X2 which contains 2 per cent divinylbenzene. Very low crosslinked resins of this type are highly swollen, soft, and easily deformed.

C. Reproducibility of Data

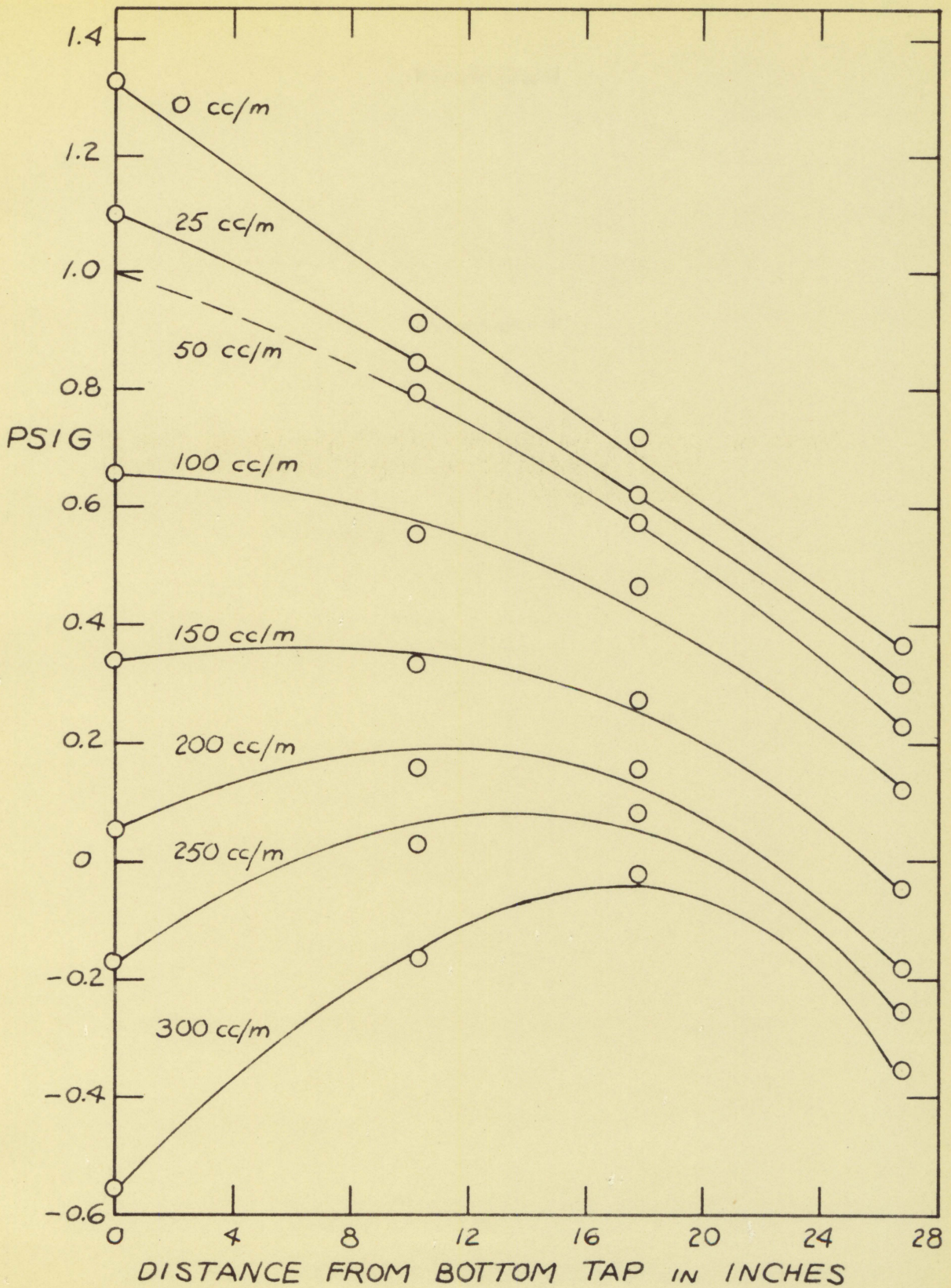
One of the problems in this study was to determine the operating conditions under which pressure drop data could be reproduced. The main factor affecting reproducibility was density of the resin bed. As mentioned in the preceding section, the resin bed becomes more tightly packed as flow increases. The change in packing density does not occur simultaneously throughout the column. The graphs in Figure 8 show gauge pressure as a

Figure 7. Change in Height of Resin Bed vs. Flow Rate for
Dowex 50M-X2, 50-100 Mesh



DE

Figure 8. Pressure vs. Distance from Bottom Tap for Flow of Distilled Water Across Dowex 50W-X2, 50-100 Mesh, Using Effluent Pump



function of distance from the bottom pressure tap for several flow rates. In this series the pressure was measured about five minutes after establishing each new flow rate. Liquid was drawn through the column by a pump.

The pressures at the top and bottom of the column were most sensitive to changes in flow rate. At no flow the pressure-position graph was linear. As flow was increased from 0 to 300 cubic centimeters per minute the pressure-position graphs deviated further from linearity. At 300 cubic centimeters per minute the pressure was a minimum at the bottom tap, rose to a maximum at the second tap from the top, and dropped again at the top tap. The decrease in pressure with increasing flow rate at the top tap was especially noticeable.

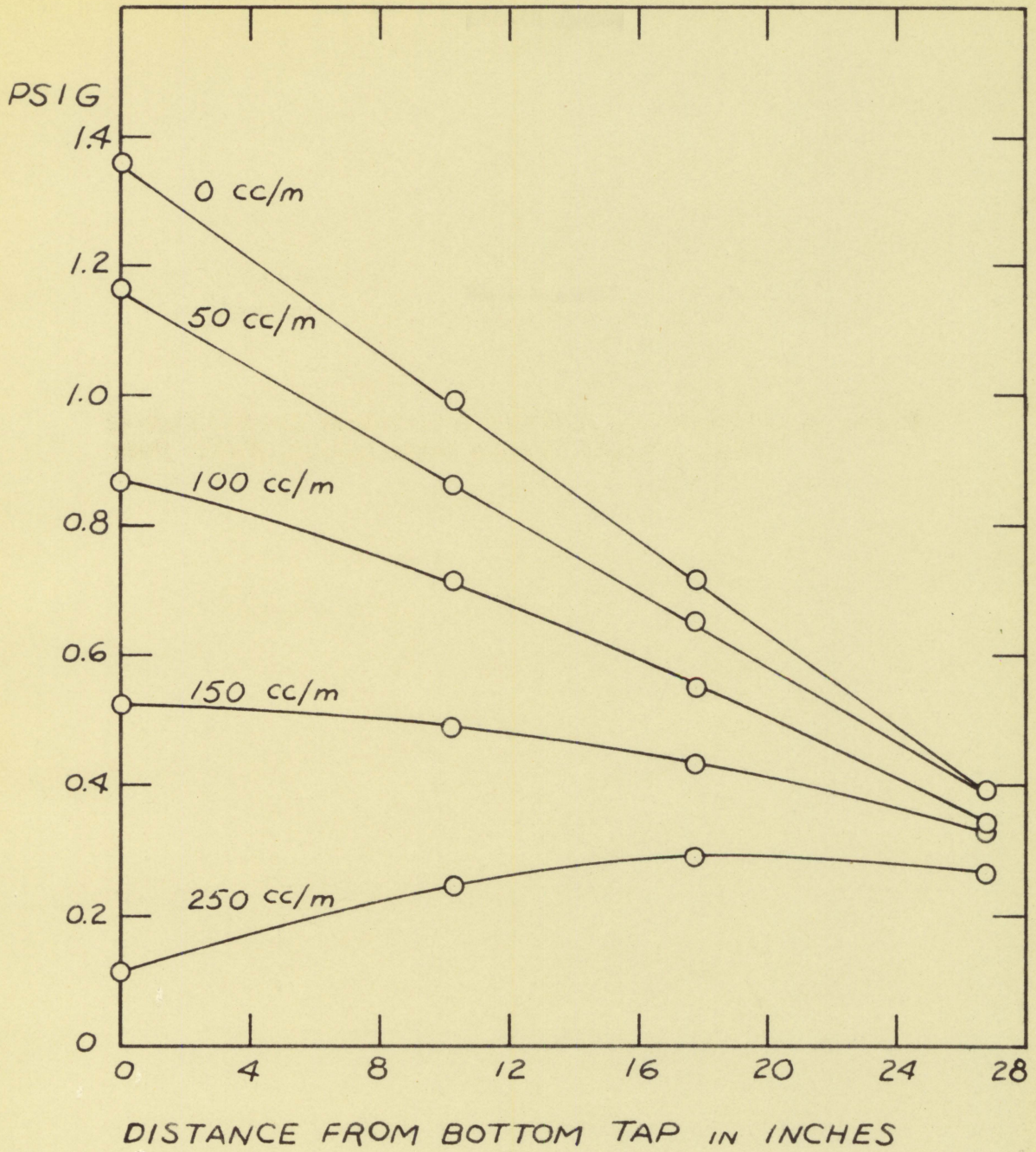
The graphs in Figure 9 also show gauge pressure in the column as a function of distance from the bottom pressure tap. In this series the pressures were measured fifteen minutes after establishing each new flow rate. The curves thus obtained were almost linear, and the change in pressure with flow rate at each tap was proportional to the height of packing above the tap.

D. Pressure Drop Across the Bed

According to Leva (20) the variables that determine the pressure drop through a packed system may be classed into two groups:

1. Variables related to the fluid passing the bed
 - (a) Fluid mass velocity
 - (b) Fluid density
 - (c) Fluid viscosity
2. Variables related to the character of the packed bed
 - (a) Voidage of the bed and particle orientation

Figure 9. Pressure vs. Distance from Bottom Tap for Flow of
Water, pH 2.85, Across Dowex 50W-X2, 50-100 Mesh



- (b) Shape of the particles
- (c) Diameter of the particles and the vessel
- (d) Surface roughness of the particles

In this study the first group of variables can be measured. The difficulty lies in evaluating the second group. The general characteristics of the bed were:

1. The particles had greater than 85 per cent sphericity.
2. The particles were porous.
3. The diameters of the dry particles ranged from 0.0059 inch to 0.0117 inch.
4. The resin swelling factor was 1.9.
5. The resin bed was compressible.
6. The resin bed was about 30 inches deep.
7. The inside diameter of the column was 3.50 inches.

The modified Reynolds number generally used in pressure drop correlations is defined as:

$$N_{Re} = \frac{D_p G}{\mu}$$

where N_{Re} = modified Reynolds number,

D_p = particle diameter, in feet,

G = fluid mass velocity, in pounds per second per square foot,

μ = fluid viscosity, in pounds per foot per second.

The maximum flow rate considered here was 300 cubic centimeters per minute which corresponded to a modified Reynolds number of 0.00162. Thus the flow rates were well within the laminar range.

The Kozeny-Carman type equation is commonly used for predicting pres-

sure drop in fixed beds. For laminar flow the equation is:

$$\frac{\Delta P}{L} = \frac{200G\mu L(1-\epsilon)^2}{D_p^2 \phi_s^2 \rho g_c \epsilon^3}$$

where $\frac{\Delta P}{L}$ = pressure drop per unit height of packing, in pounds per square inch per foot of resin,

G = fluid mass velocity, in pounds per second per square foot,

μ = fluid viscosity, in pounds per foot per second,

ϵ = bed voidage = $\frac{\text{volume of voids}}{\text{volume of bed}}$,

D_p = particle diameter, in inches,

ϕ_s = bed shape factor,

ρ = fluid density, in pounds per cubic foot,

g_c = acceleration of gravity, 32.2 feet per second per second.

The only factor in this equation which could not be measured accurately in this case was the bed voidage.

The graph in Figure 10 shows average pressure drop per foot of resin as a function of flow rate. The fluid is distilled water. The graph is linear and may be described by the equation:

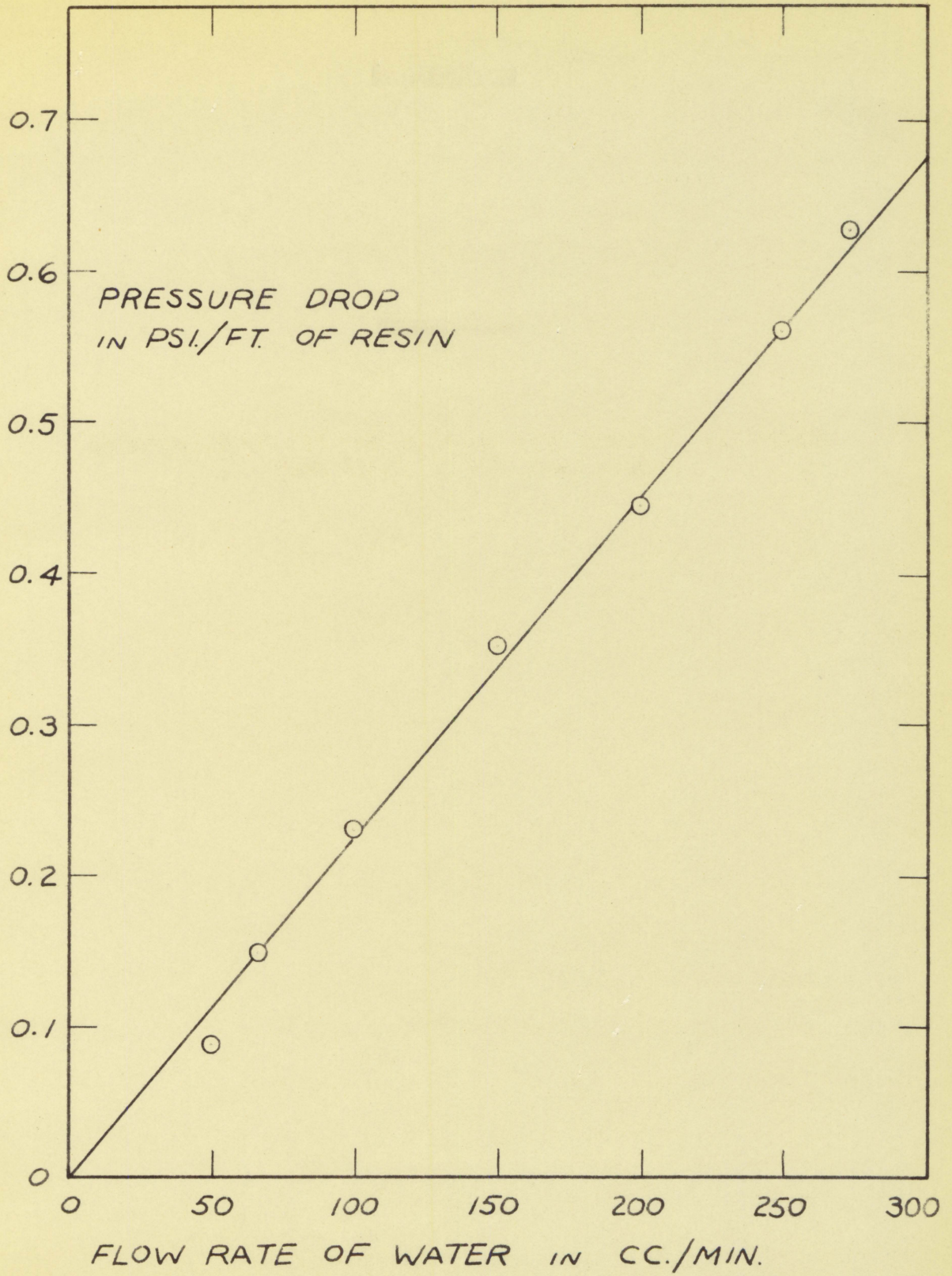
$$\frac{\Delta P}{L} = 2.27 \times 10^{-3} v$$

where $\frac{\Delta P}{L}$ = pressure drop per unit height of packing, in pounds per square inch per foot of resin,

v = fluid velocity, in cubic centimeters per minute.

The measured pressure drop may be substituted in the Kozeny-Carman equation to solve for ϵ , the bed voidage. The bed voidage thus calculated is 0.77. This value does not agree with the voidage value of 0.064 calcu-

Figure 10. Pressure Drop vs. Flow Rate for Distilled Water
Across Dowex 50W-X2, 50-100 Mesh



lated from the known weight of resin in the column.¹ The actual voidage should be rather small because the particle sizes vary, and the smaller spheres will fill spaces between the larger ones. Leva et al. (21) show bed voidage as a function of D_p/D_t for smooth mixed spheres. D_p/D_t is the ratio of particle diameter to column diameter. In this case where $D_p/D_t = 0.0048$ the voidage should be less than 0.10.

If a voidage of 0.10 is used in the Kozeny-Carman equation the calculated pressure drop is 6500 pounds per square inch per foot of resin. Evidently this type of pressure drop correlation does not apply in its present form to flow across a packed bed of ion-exchange resin.

E. Variation of Pressure Drop with pH

The graphs in Figure 11 show pressure drop per foot of resin as a function of flow rate for four values of pH. As pH was decreased from 7.0 to 1.0 the slope of the graph increased about 13 per cent. Sulfuric acid was used to increase the acidity, and the increased viscosity of the solution probably accounted for the greater pressure drop.

The photomicrographs in Figure 12, 13, and 14, show fresh resin in a solution of pH 7, fresh resin in a solution of pH 1, and used resin in solution of pH 1. The change in pH had no effect on the external shape of the fresh resin. The used resin showed some effects of wear and deformation. Attrition of particles in the column will account for some increase in pressure drop over a period of time.

¹See calculations in Appendix A.

Figure 11. Pressure Drop vs. Flow Rate for Water of Different pH Values Across Dowex 50W-X2, 50-100 Mesh

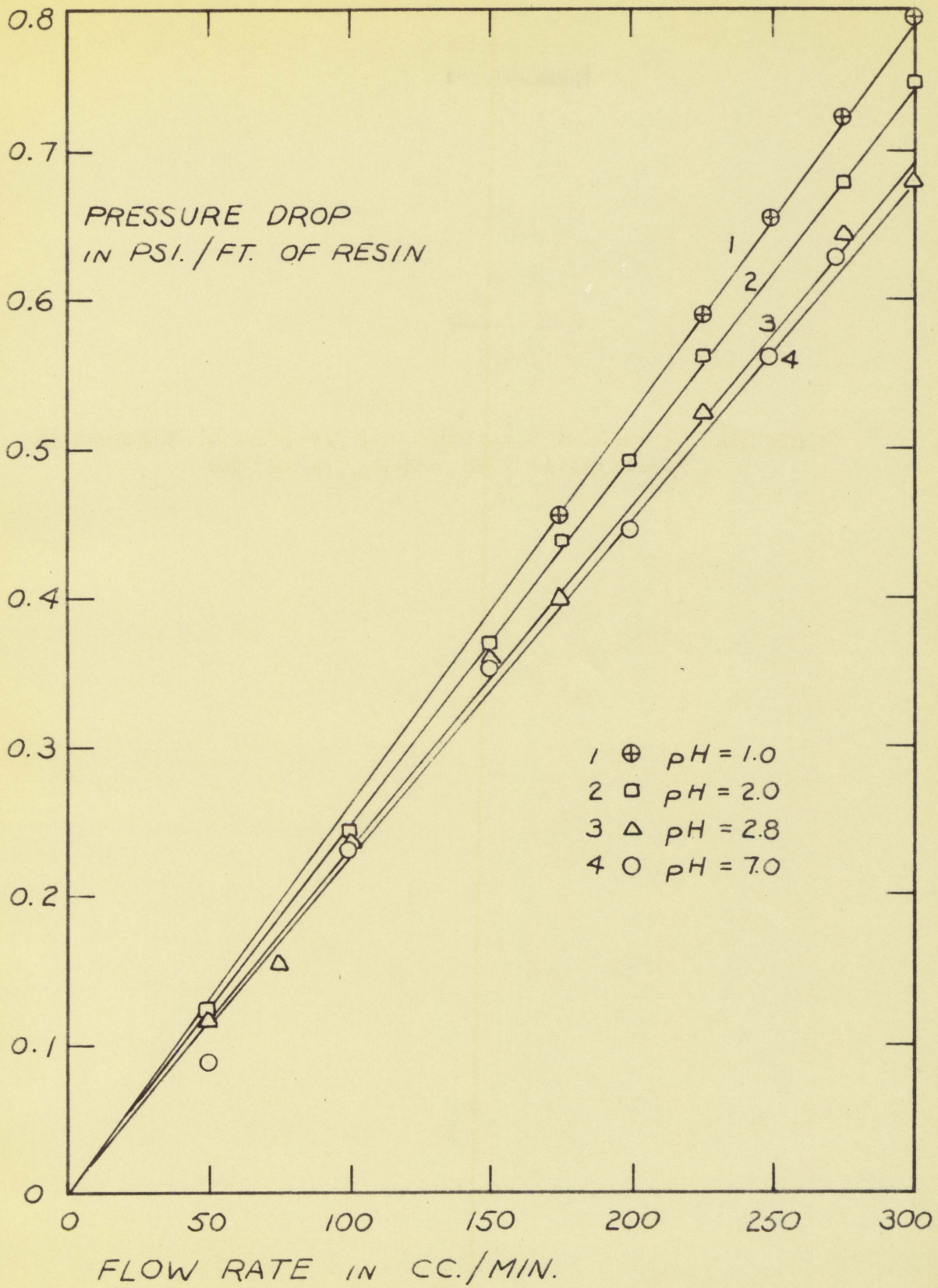


Figure 12. Fresh Dowex 50W-X2 Resin 50-100 Mesh, in Distilled Water, x 55

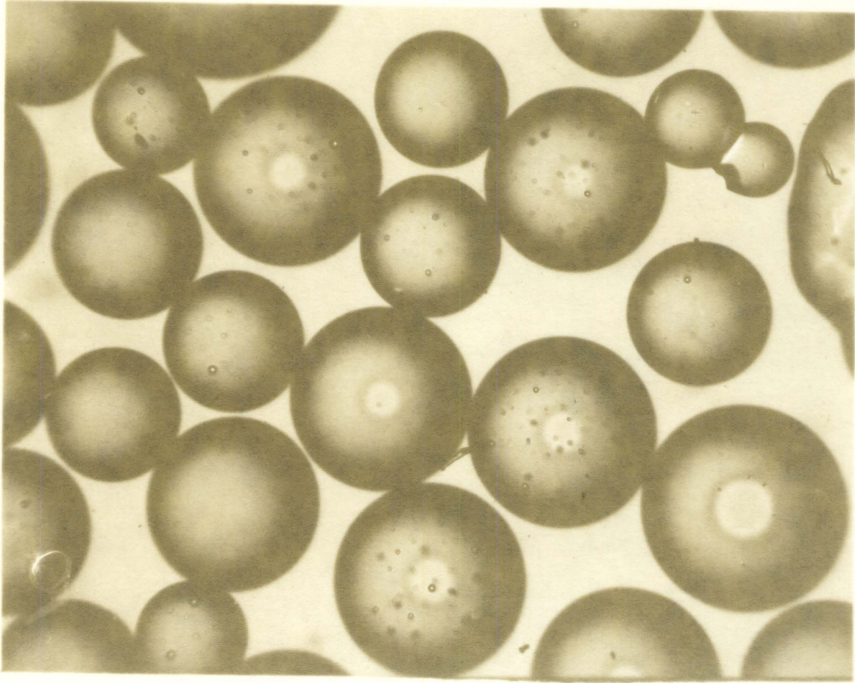


Figure 13. Fresh Dowex 50W-X2 Resin, 50-100 Mesh, in Aqueous Solution, pH 1.0, x 55

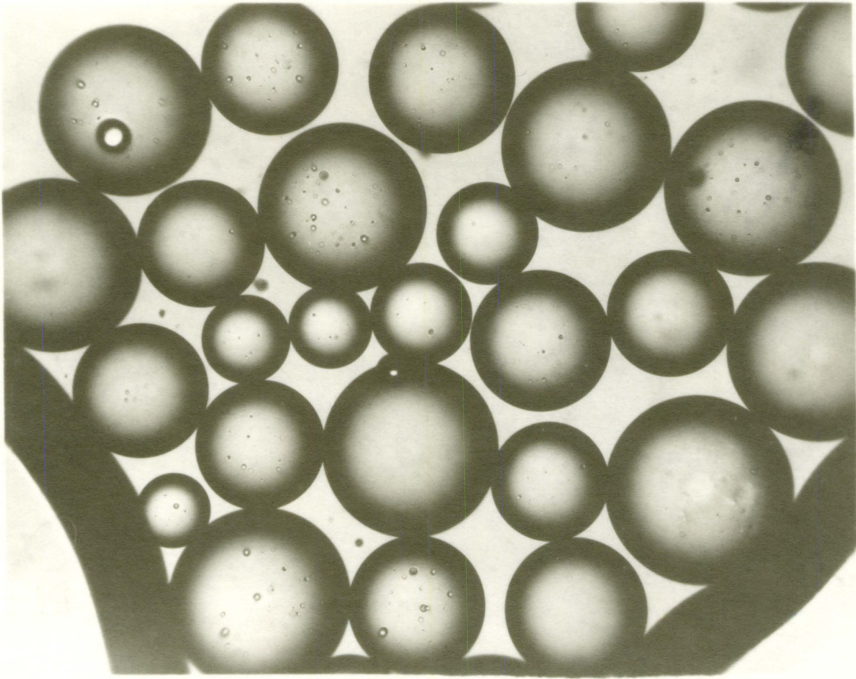
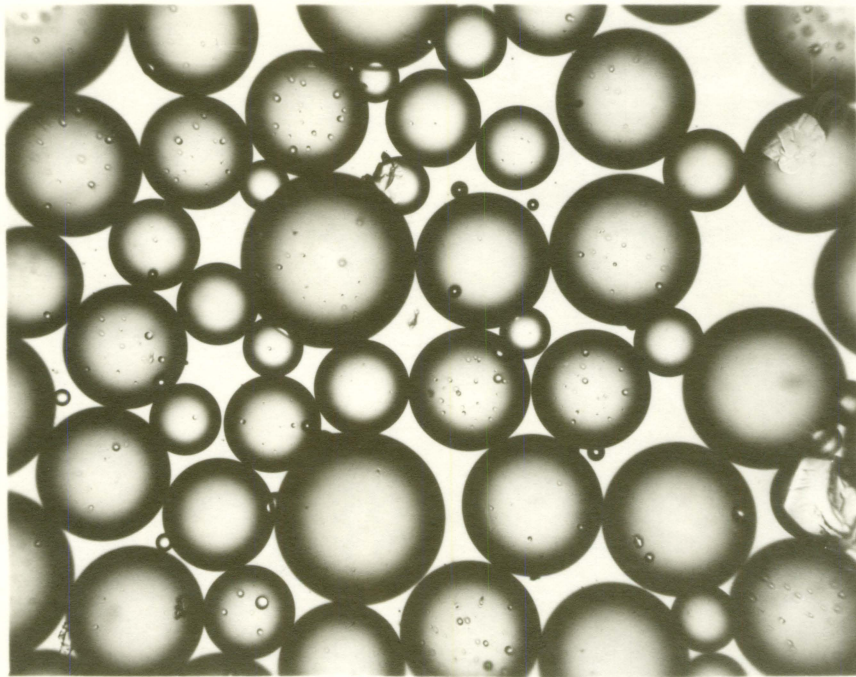


Figure 14. Used Dowex 50W-X2 Resin, 50-100 Mesh, in Aqueous Solution, pH 1.0, x 55



VII. CONCLUSIONS AND RECOMMENDATIONS

The conclusions resulting from this study were:

1. The resin bed was compressible and became more tightly packed as flow rate increased.
2. A definite period of time was required for the packed bed to become stabilized with a new flow rate. In the case of a column 3.50 inches in inside diameter and packed 30 inches deep with 50-100 mesh Dowex 50W-X2 resin the minimum time required to reach equilibrium was about 15 minutes.
3. The average relationship between pressure drop and fluid flow rate for distilled water between 0 and 300 cubic centimeters per minute was:

$$\frac{\Delta P}{L} = 2.27 \times 10^{-3} v$$

where $\frac{\Delta P}{L}$ = pressure drop per unit height of packing, in pounds per square inch per foot of resin,

v = fluid velocity, in cubic centimeters per minute.

The Kozeny-Carman type equation did not give a good prediction of pressure drop in this case.

4. The pressure drop per unit height of bed increased slightly as pH was decreased from 7.0 to 1.0 by adding concentrated sulfuric acid to the distilled water.

A better correlation of pressure-drop data requires further studies with resins of various sizes. The 4-inch column used in this study should not be charged with resins smaller than 100-mesh because the small particles pass through the screens and plug the lines, rotameters, and pump. It will probably operate best with standard 20-50 mesh resin.

An accurate means of determining bed voidage is needed. Microscopic examination of the resins may be helpful in this respect.

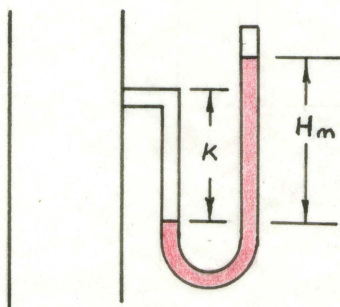
VIII. BIBLIOGRAPHY

1. Allen, H. V. Pressure drop for flow through beds of granular absorbents. *Petroleum Refiner* 23: 247-252. 1944.
2. Blake, F. C. The resistance of packing to fluid flow. *Trans. Am. Inst. Chem. Eng.* 14: 415-421. 1922.
3. Boussinesq, M. J. Sur la theorie de la transpiration des gaz a travers les milieux poreux. *Comptes Rendus* 159: 390-394. 1914.
4. _____. Evaluation approximative de la constante de filtration, pour un milieu filtrant constitue par des grains spheriques d'un diametre donne. *Comptes Rendus* 159: 519-525. 1914.
5. Carman, P.C. Fluid flow through granular beds. *Trans. Inst. Chem. Eng. (London)*. 15: 150-166. 1937.
6. Chalmers, J., Taliaferro, D. B. and Rawlins, E. L. Flow of air and gas through porous media. *Trans. Am. Inst. Min. and Met. Eng., Petrol. Div.* 98: 355-400. 1932.
7. Chilton, T. H. *The science of petroleum*. London, Oxford Univ. Press. 1938.
8. _____ and Colburn, A.P. Pressure drop in packed tubes. *Ind. Eng. Chem.* 23: 913-931. 1931.
9. D'Arcy, H.P.G. *Les fontaines publiques de la ville de Dijon*. Paris, Victor Dalmont. 1856. (Original not available for examination; cited in Leva et al. (21, p.3).)
10. Dow Chemical Company. *Dowex: Ion exchange*. Chicago, Lakeside Press. 1958.
11. Dupuit, A. J. *Etudes theoriques et pratiques sur le mouvement des eaux dans les canaux decouverts et a travers les terrains permeables*. Paris, Victor Dalmont. 1863. (Original not available for examination; cited in Boussinesq (3, p. 524).)
12. Ergun, S. Determination of particle density of crushed porous solids. *Ind. Eng. Chem. Anal. Ed.* 23: 151-156. 1951.
13. Fancher, G. H. and Lewis, J. A. Flow of simple fluids through porous materials. *Ind. Eng. Chem.* 25: 1139-1147. 1933.
14. Furnas, C. C. *The flow of gases through beds of broken solids*. U. S. Bureau of Mines Technical Paper 307. 1929.

15. Hatch, L. P. Flow of fluids through granular materials. Trans. Am. Geophys. Union 24: 537-547. 1943.
16. Hatfield, M. R. Fluid flow through porous carbon. Ind. Eng. Chem. 31: 1419-1424. 1939.
17. Kahn, M., Lawson, K. and Jones, K. J. Ion-exchange resins. U. S. Atomic Energy Commission Report LA-2054 UNM (Los Alamos Scientific Laboratory). (Office of Technical Services, Washington, D. C.) May 30, 1957.
18. Leva, M. Correlations in fixed bed systems. Chem. Eng. 64, No. 9: 245-248. 1957.
19. _____ . Equipment for fixed and moving beds. Chem. Eng. 64, No. 7: 258-262. 1957.
20. _____ . Variables in fixed bed systems. Chem. Eng. 64, No. 8: 263-266. 1957.
21. _____ . Weintraub, M., Grummer, M., Pollehek, M. and Storch, H.H. (Fluid flow through packed and fluidized systems.) U. S. Bureau of Mines Bulletin 504. 1951.
22. Martin, J. J., McCabe, W. and Monrad, C. C. Pressure drop through stacked spheres. Chem. Eng. Prog. 47: 91-94. 1951.
23. Meyer, W. G. and Work, L. T. Flow of fluids through beds of packed solids. Trans. Am. Inst. Chem. Eng. 33: 13-33. 1937.
24. Nachod, F. C. and Schubert, J. Ion exchange technology. New York, Academic Press, Inc. 1956.
25. Schwartz, G. W. and Smith, J. M. Flow distribution in packed beds. Ind. Eng. Chem. 45: 1209-1218. 1953.
26. Von Emersleben, O. Das D'Arcy'sche Filtergesetz. Physikalische Zeitschrift 26: 601-610. 1925.
27. Waddell, H. The coefficient of resistance for solids of various shapes. J. Franklin Inst. 217: 459-470. 1934.
28. White, A. M. Pressure drop and loading velocities in packed towers. Trans. Am. Inst. Chem. Eng. 31: 390-408. 1935.
29. Zeisberg, F. C. The resistance of absorption tower packing to gas flow. Trans. Am. Inst. Chem. Eng. 12, Part II: 231-237. 1919.

IX. APPENDIX

A. Sample Calculations

1. Gauge Pressure from Manometer Reading

$$P_A = \frac{62.4 \text{ lb./ft.}^3}{144 \text{ in./ft.} \times 2.54 \text{ cm./in.} \times 12 \text{ in./ft.}} (H_m \rho_m - K \rho_A) \text{ cm.}$$

$$\rho_m = 2.495 \text{ gm./cc.}$$

$$\rho_A = 1.00 \text{ gm./cc.}$$

$$\text{If } H_m = 65.81 \text{ cm., } K = 141.8 \text{ cm.}$$

$$\begin{aligned} \text{Then } P_A &= 0.0142 (65.81 \times 2.495 - 141.8 \times 1.00) \\ &= 0.0142 (22.4) = \underline{\underline{0.296}} \text{ psig.} \end{aligned}$$

2. Modified Reynolds Number

$$NR_e = \frac{D_p G}{\mu}$$

$$D_p = \text{Average between 50 and 100 mesh}$$

$$= (0.0117 + 0.0059) \frac{1}{2} = 0.0088 \text{ inch dry}$$

From Dow Chemical Company (10), p. 13;

Swollen resin diam. = 1.9

Dry copolymer diam.

$$D_p = \frac{0.0088 \times 1.9}{12} = \underline{\underline{0.0014}} \text{ ft. average}$$

$$G = 300 \text{ cc./m.} \times \frac{1}{0.0668 \text{ ft.}^2} \times 1.00 \text{ gm./cc.} \times \frac{1}{453} \frac{\text{lb.}}{\text{gm.}} \times \frac{1}{60} \frac{\text{min.}}{\text{sec.}}$$

$$= 0.165 \text{ lb./sec.} \cdot \text{ft.}^2$$

$$\mu = 0.958 \text{ cp.} = 0.1425 \text{ lb./ft.} \cdot \text{sec.}$$

$$N_{Re} = \frac{0.0014 \text{ ft.} \times 0.165 \text{ lb./sec.} \cdot \text{ft.}^2}{0.1425 \text{ lb./sec.} \cdot \text{ft.}} = \underline{\underline{0.00162}}$$

Flow is laminar for $N_{Re} < 10$.

3. Bed Voidage

$$\epsilon = \frac{\text{total packed vol.} - \text{vol. of resin}}{\text{total packed vol.}}$$

$$\text{Total volume} = 9.62 \text{ in.}^2 \times (2.54)^2 \frac{\text{cm.}^2}{\text{in.}^2} \times 78 \text{ cm.}$$

$$= 4840 \text{ cm.}^3$$

$$\text{Volume of resin} = (12 \text{ lb.} \times \frac{1 \text{ lb.}}{22 \text{ kg.}} - 1.83 \text{ kg.}) \times \frac{1 \text{ ft.}^3}{50 \text{ lb.}} \times \frac{1 \text{ cc.}}{0.0160 \text{ gm.}}$$

$$= 4530 \text{ cm.}^3$$

$$\therefore \epsilon = \frac{4840 - 4530}{4840} = 0.064 = 6.4\%$$

4. Kozeny-Carman Equation

$$\Delta P = \frac{200 G \mu L (1 - \epsilon)^2}{D_p^2 \phi_s^2 \rho \epsilon_c \epsilon^3}$$

$$\frac{\Delta P}{L} = \frac{200 G \mu (1 - \epsilon)^2}{D_p^2 \phi_s^2 \rho \epsilon_c \epsilon^3}$$

$$\frac{\Delta P}{L} = 0.680 \text{ psi./ft.}$$

$$G = 0.165 \text{ lb./sec.} \cdot \text{ft.}^2$$

$$\mu = 0.1425 \text{ lb./ft.} \cdot \text{sec.}$$

$$D_p = 0.0168 \text{ in.}$$

$$\phi_s^2 = (1.00)^2 = 1.00$$

$$\rho = 62.4 \text{ lb./ft.}^3$$

$$\epsilon_c = 32.2 \text{ ft./sec.}^2$$

$$0.680 = \frac{200 \times 0.165 \times 0.1425 (1 - \epsilon)^2}{(0.0168)^2 \times (1.00) \times 62.4 \times 32.2 \times \epsilon^3}$$

$$\frac{(\epsilon)^3}{(1 - \epsilon)^2} = 8.28$$

$$\therefore \epsilon = 0.77$$

B. Data for Graphs

1. Data for Change in Height of Resin Bed vs. Flow Rate Graph, Figure 7.

Flow Rate cc./m.	H ₀ cm.
0	0
50	-1.40
100	-2.10
125	-2.00
150	-2.55
175	-2.75
200	-3.10
225	-3.00
250	-3.00
275	-3.25
300	-3.45

2. Data for Pressure Drop vs. Flow Rate Graphs Figures 8 and 9

pH = 7.0		pH = 2.8		pH = 2.0		pH = 1.0	
Flow Rate	P _o /ft.	Flow Rate	P _o /ft.	Flow Rate	P _o /ft.	Flow Rate	P _o /ft.
cc./m.	psi./ft.	cc./m.	psi./ft.	cc./m.	psi./ft.	cc./m.	psi./ft.
50	0.087	50	0.117	50	0.121	50	0.121
66	0.150	75	0.154	100	0.241	100	0.238
86	0.190	100	0.233	150	0.369	150	0.360
100	0.230	125	0.271	175	0.438	175	0.455
150	0.352	150	0.361	200	0.492	200	0.490
200	0.445	175	0.402	225	0.562	225	0.590
250	0.561	225	0.521	250	0.560	250	0.654
272	0.627	250	0.565	275	0.678	275	0.720
287	0.721	275	0.643	300	0.750	300	0.791
		300	0.679				